Modelling Earth's magnetic field over the South Atlantic Anomaly region using *Swarm* satellite and ground-based data

Sanele Lionel Khanyile[1,2]*, Emmanuel Nahayo[1], and John Bosco Habarulema[1,2,3]

[1]South African National Space Agency (SANSA), Hospital Street, Hermanus 7200, South Africa

[2]Department of Physics and Electronics, Rhodes University, Makhanda 6140, South Africa

[3]Centre for Space Research, North-West University, Potchefstroom 2520, South Africa

Tel: +27 28 285 0077, Email address: skhanyile@sansa.org.za

Outline

- Introduction
- Data selection and processing
- Methodology (Revised Spherical Cap Harmonic Analysis (R-SCHA))
- Results and discussions
- Conclusion

Introduction

- The South Atlantic Anomaly (SAA), located between Southern Africa and South America, is a key region of interest due to its notably weak magnetic field, which impacts satellite operations, increases radiation exposure, and affects space weather (Konradi et al., 1994; Gubbins et al., 2000, 2000b; Smith et al., 2016).

- Recent studies using global models like IGRF-13 (Rother et al., 2021) and CHAOS-7 (Finlay et al., 2020) show that the SAA is deepening, expanding, and moving westward due to complex core processes. However, these models may miss fine-scale features, highlighting the need for detailed regional studies.

- This study models the Earth's magnetic field over the SAA using high-resolution *Swarm* satellite data (Olsen et al., 2013) and ground-based observations. Applying the R-SCHA technique, it aims to better understand the region’s ongoing magnetic field intensity decrease.

Introduction (cont.)

Geomagnetic field intensity over the SAA region from the CHAOS-8.5 model at epoch 2024.0 (ground level), highlighting the study area, data coverage (green circles), and the modelled region (blue circles).

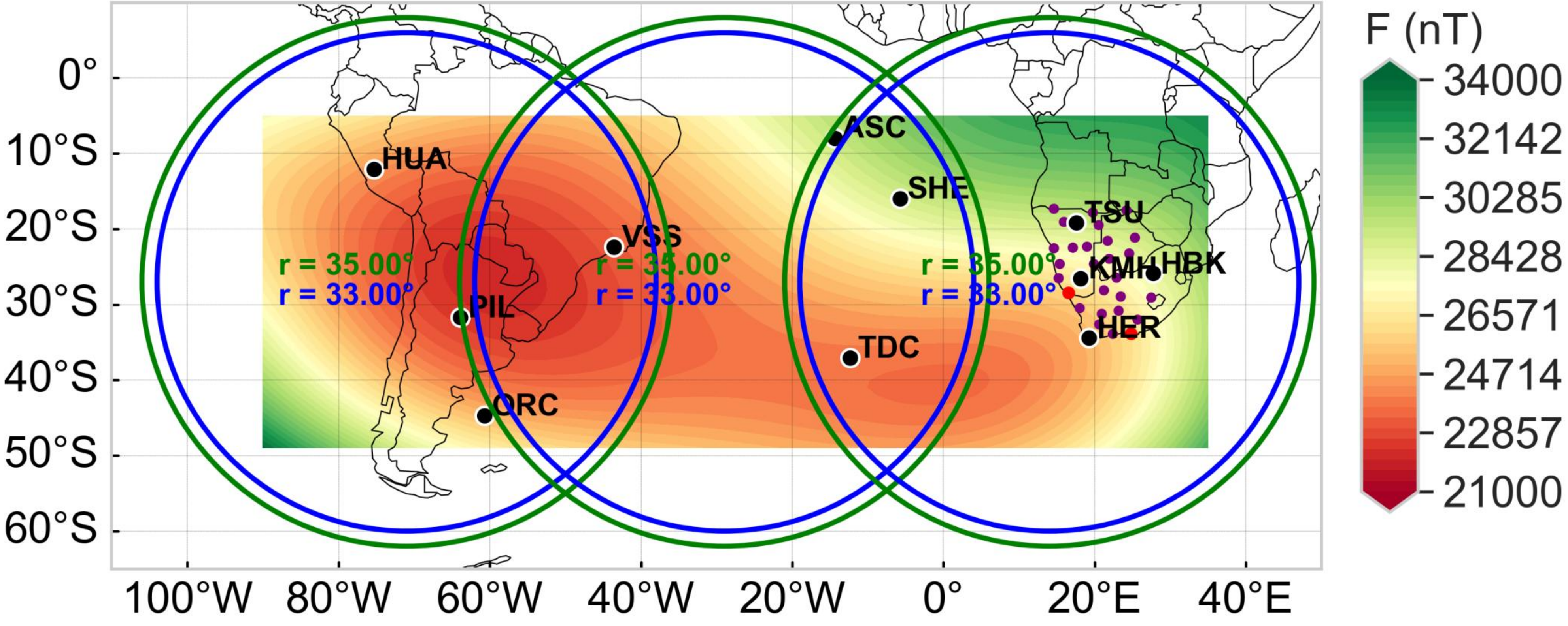

Model 3 Model 2 Model 1

Data selection and processing

- Data Source: Used *Swarm* satellite data (2014-2024) from satellites Alpha, Bravo, and Charlie (Olsen et al., 2013).
- Region Focus: Selected data for latitudes 8°N to 62°S and longitudes 106°W to 49°E, to model the region of latitudes 5°S to 49°S and longitudes 90°W to 35°E.
- Time Selection: Only quiet night-time measurements were used, defined as those taken when the Sun forms an angle with the horizon smaller than -10°.
- Filtering Criteria selects geomagnetically quiet periods: Retained data with Kp ≤ 2, |Dst| ≤ 20 nT/h, |dDst/dt| ≤ 3 nT/h, and |dRC/dt| ≤ 3 nT/h.
- Lithospheric Magnetic Field: Removed using the MF7 lithospheric field model (Maus, 2010).
- The external field contributions: Removed using the CHAOS-8.5 global geomagnetic field model (Kloss et al., 2026).
- Data Decimation: Reduced model input data by retaining only data recorded inside 0.2° radius bins on the grid of 1° X 1°, and retaining a single point per epoch, resulting in 84,664 for model 1, 84,479 for model 2, and 84,571 for model 3 vector data points.

Data selection and processing (cont.)

- Data Source: Used hourly mean data from eleven magnetic observatories: (TSU, HBK, KMH, HER, SHE, ASC, TDC, VSS, ORC, PIL, HUA) 2014 - 2024.

- Selection Criteria: Applied the same criteria as for satellite data selection.

- Daily Averaging: Daily means were calculated by averaging the selected hourly data.

- Data Retained: A total of approximately 3,127 vector data points per station were retained from the observatory data. A total of 135 vector data points were retained from the survey stations.

- Crustal Bias Removal: Removed biases from the observatory and survey using methods by Korte and Thebault (2007); Mandea and Langlais (2002). Biases (Xc, Yc, Zc) were calculated as differences between observatory measurements (Xi, Yi, Zi) and model predictions (Xm, Ym, Zm) using the CHAOS-8.5 model.

Methodology R-SCHA

In the R-SCHA method (Thébault et al., 2006), the scalar potential field V is given by the equation below:

$$V(r,\theta,\varphi,t) = R\sum_{m=0}^{K_{int}}\sum_{k=0}^{k}\left(\frac{R}{r}\right)^{n_{k(m)}+1}\left[g_{i,n_{k(m)}}^{m}(t)\cos(m\varphi) + h_{i,n_{k(m)}}^{m}(t)\sin(m\varphi)\right]P_{n_{k(m)}}^{m}(\cos\theta) +$$
$$\mathrm{R}\sum_{k=1}^{K_{ext}}\sum_{m=0}^{k}\left(\frac{r}{R}\right)^{n_{k(m)}}\left[g_{e,n_{k(m)}}^{m}(t)\cos(m\varphi) + h_{e,n_{k(m)}}^{m}(t)\sin(m\varphi)\right]P_{n_{k(m)}}^{m}(\cos\theta) +$$
$$R\sum_{p=1}^{P_{max}}\sum_{m=0}^{m}R_p(r)\left[g_p^m(t)\cos(m\varphi) + h_p^m(t)\sin(m\varphi)\right]K_p^m(\cos\theta) +$$
$$R\sum_{p=1}^{M_{max}}\sum_{m=0}^{m}R_0(r)[g_0^m(t)\cos(m\varphi) + h_0^m(t)\sin(m\varphi)]K_0^m(\cos\theta),$$

here, *R* is the Earth's mean radius. θ *and* φ are colatitude and longitude, $P_{n_{k(m)}}^{m}(\cos\theta)$ are Legendre associated functions, $K_p^m(\cos\theta)$ are Mehler functions.

Results and discussions

Optimization of Legendre Expansion Limits K_{max} and M_{max} and the Mehler Conical Function P_{max}, using half angle 35°.

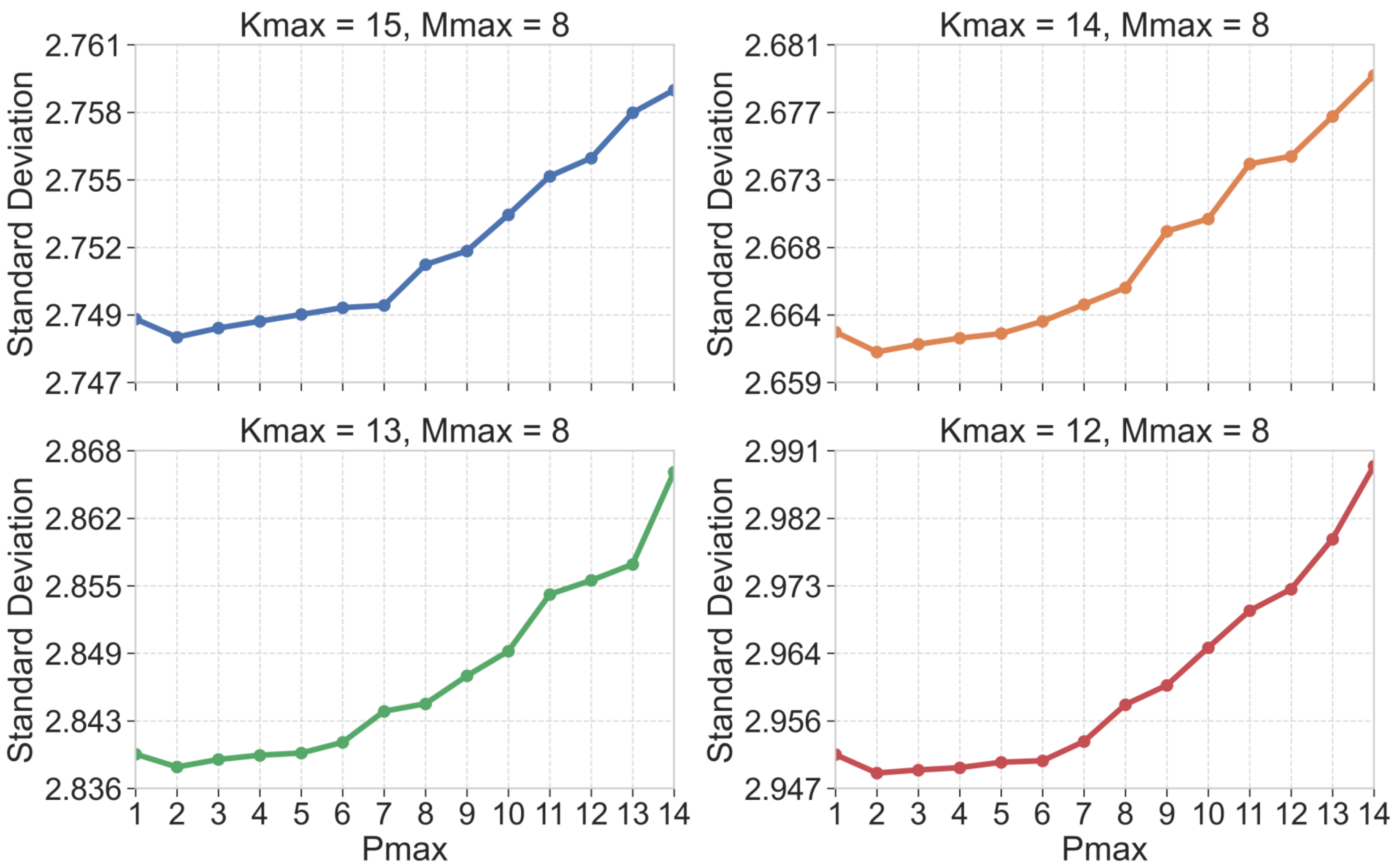

Results and discussions (cont.)

Ground-level (0 km) differences between the developed model and CHAOS-8.5 at epoch 2019.0.

R-SCHA

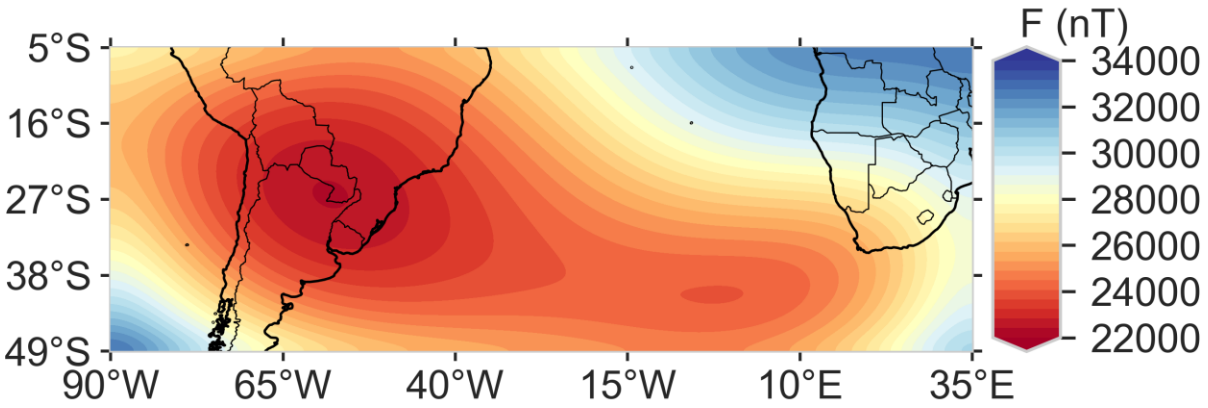

CHAOS-8.5

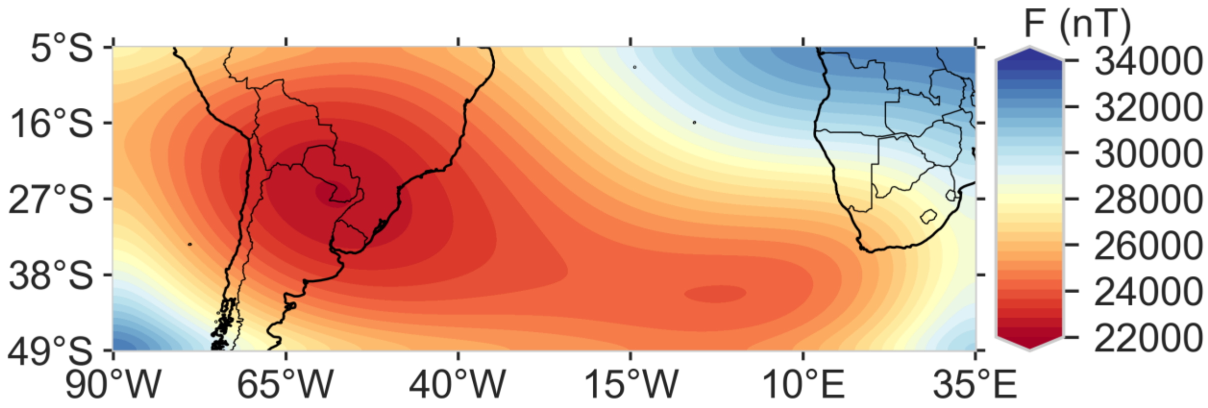

Differences

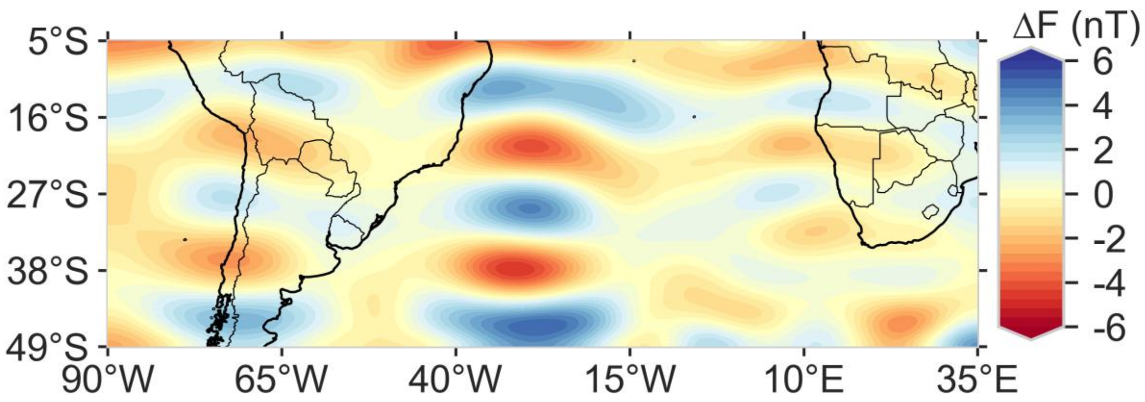

Results and discussions (cont.)

Total geomagnetic field change between epochs 2014.5 and 2024.5, as predicted by the developed model at ground level (0 km).

2014.5

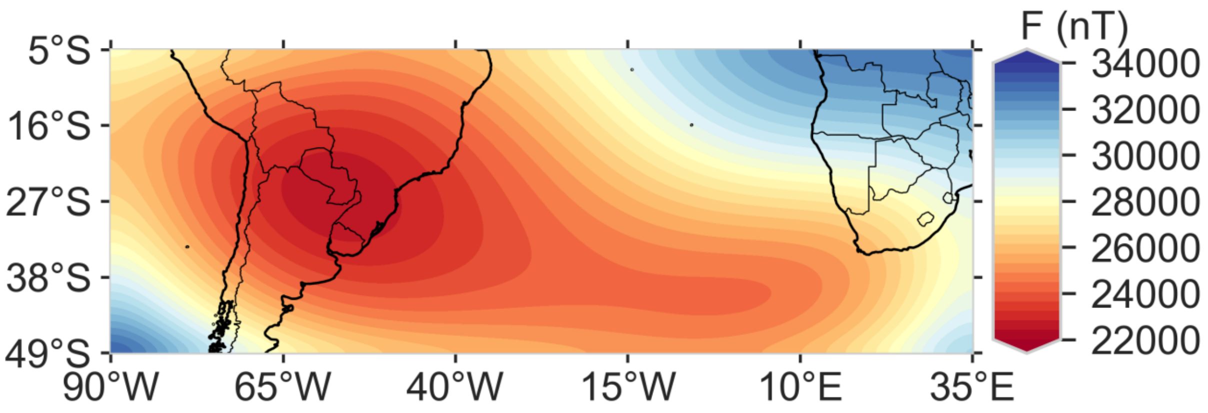

2024.5

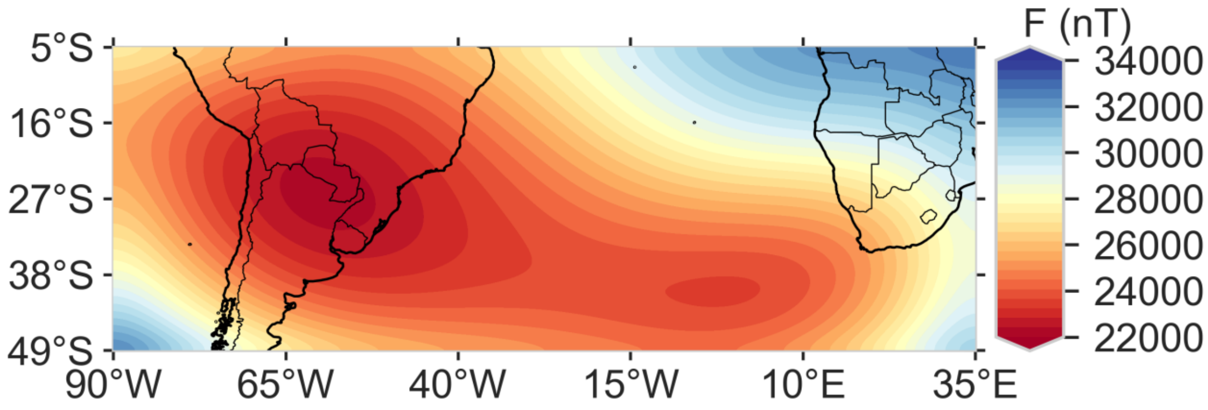

Change

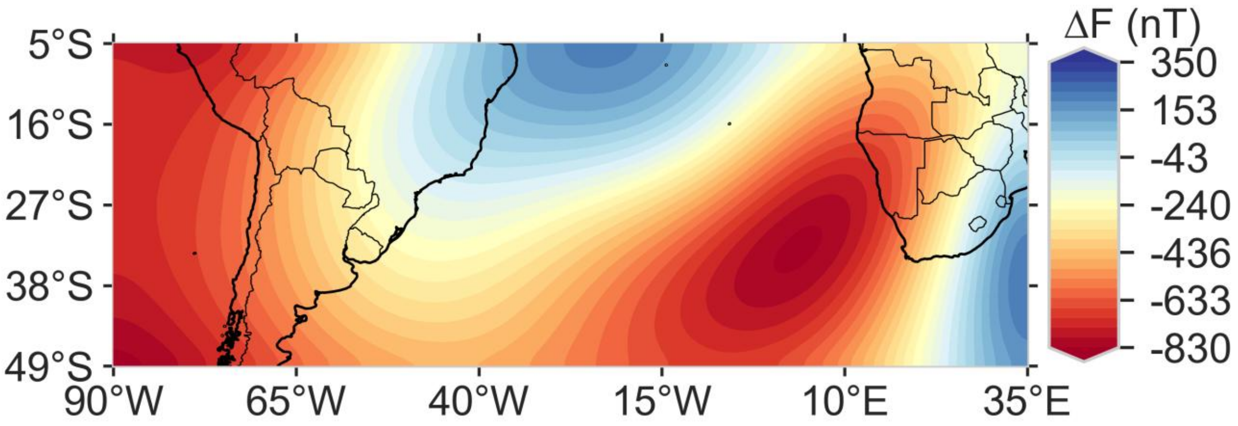

Results and discussions (cont.)

Illustration of the Geomagnetic Virtual Observatory (GVO) concept. The red dot denotes the GVO, the red star indicates a ground observatory, and the blue dashed line represents the satellite orbit.

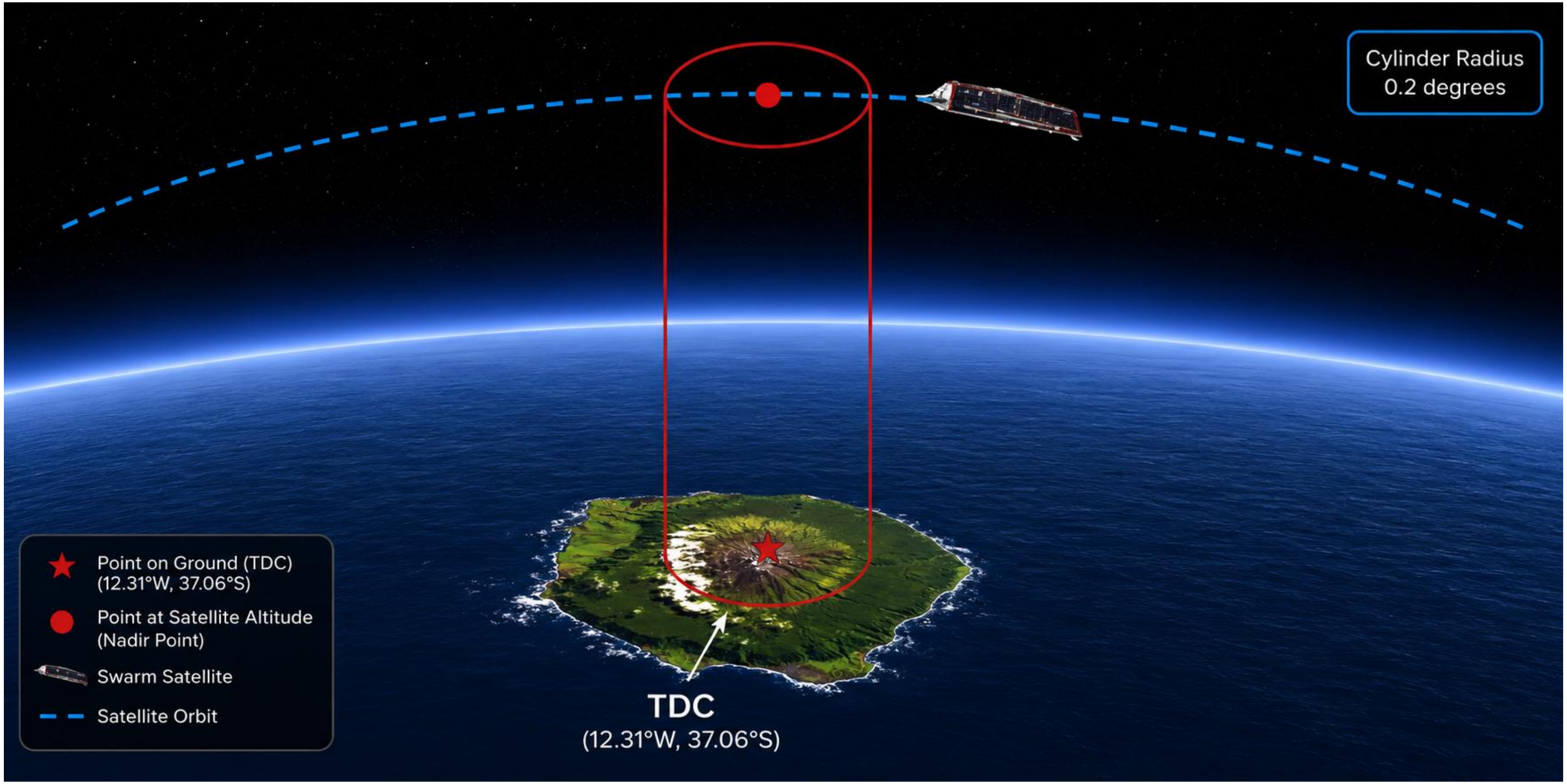

Results and discussions (cont.)

- The approach follows the methodology described by Nahayo and Korte (2022), and is expressed as:

$$D_{virtual} = D_{swarm} + (C_{virtual} - C_{swarm}),$$

here, $D_{virtual}$ represents the magnetic field value at the virtual observatory, D_{swarm} is the recorded *Swarm* satellite observation, $C_{virtual}$ is the CHAOS-8.5 model prediction at the virtual observatory position, and C_{swarm} is the CHAOS-8.5 model prediction at the original satellite observation position, all evaluated at the same epoch.

- To identify possible changes, we applied a method based on the approach described by Chulliat et al. (2010). This method examines temporal changes in the geomagnetic field by calculating the annual rate of change of the X, Y, Z, and total field F components. The Secular Variation (SV) was estimated using a centred finite difference scheme over a 12-month interval, given by:

$$dB/_{dt} = {}^{B(t+6)-B(t-6)}/_{1\,year}$$

here, B represents the monthly mean value of one geomagnetic field component *(X, Y, Z, or F)*, and t denotes the month at which the SV is centred.

Results and discussions (cont.)

- To suppress seasonal signals associated with external field sources, such as magnetospheric and ionospheric current systems, a 12-month running mean was applied to the SV time series, $\dot{B}(t)(B = X, Y, Z, or\ F)$, following the approach of Olsen and Mandea (2007).

- Over periods ranging from months to years, abrupt changes in the linear SV trend may occur. These rapid changes are known as SV impulses or geomagnetic jerks (Courtillot et al., 1978). Geomagnetic jerks are often limited in both space and time, but they can appear at different times in different regions of the world and may affect different geomagnetic field components (e.g., Mandea et al., 2010).

Results and discussions (cont.)

Comparison of SV in the X, Y, Z, and total field F components. The right panel shows SV derived from the GVO above TDC (478 km, red dots), the CHAOS-8.5 global model (blue lines), and the R-SCHA regional model (orange lines). The left panel presents ground observatory SV (black dots) together with the corresponding 12-month running means (green dots).

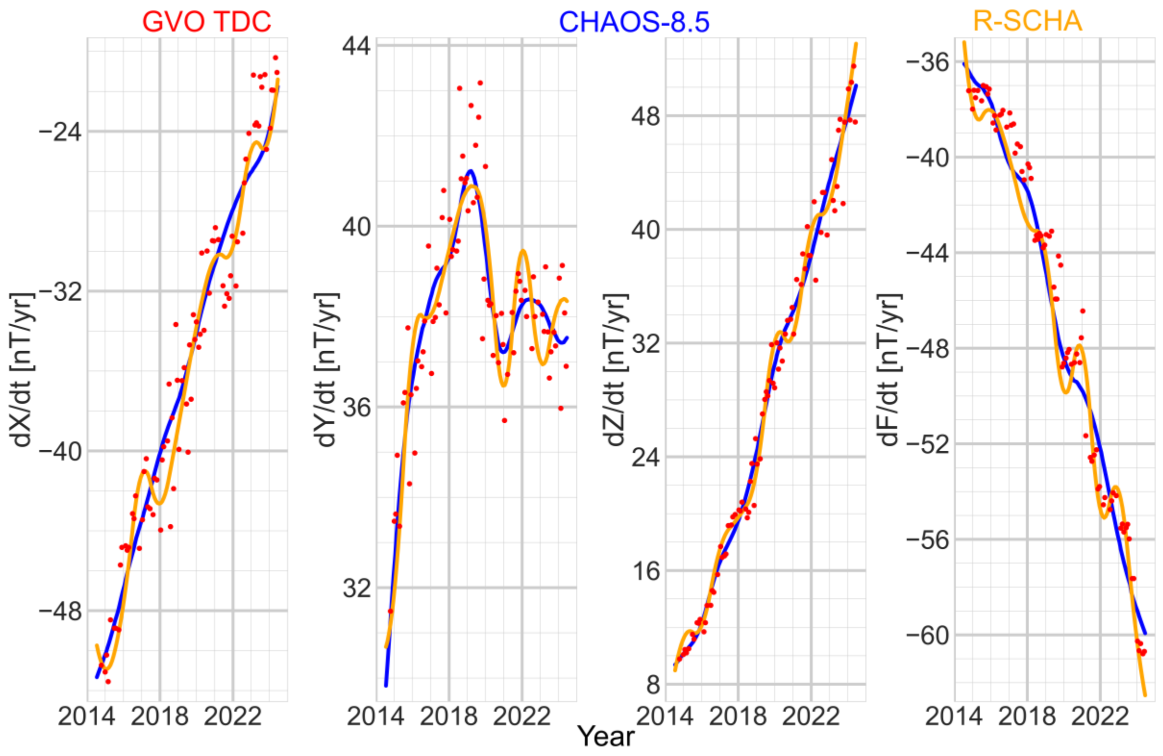

Pavón-Carrasco et al. (2021)

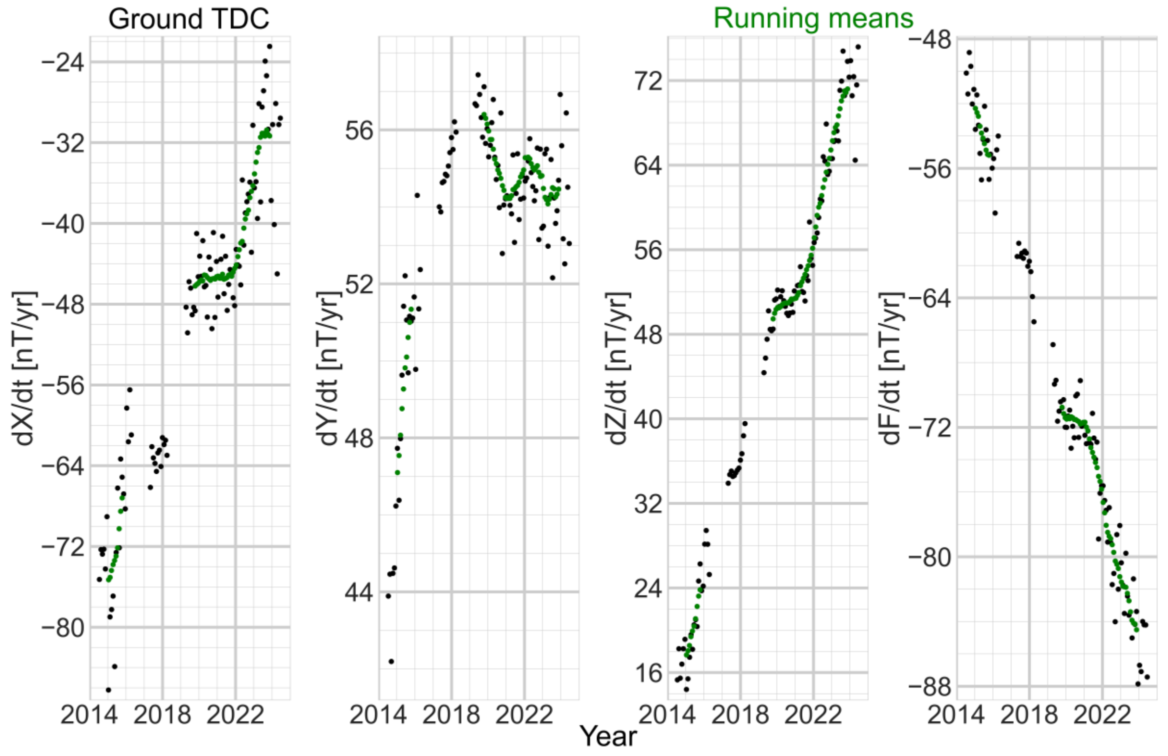

Khanyile and Nahayo (2024)

Khanyile et al. (2026)

Conclusion

- This study developed a regional geomagnetic field model based on the R-SCHA approach to investigate the evolution of the SAA between 2014 and 2024. The results successfully capture the recent spatial and temporal variability of the field within the study region.

- Importantly, the residuals between the R-SCHA regional model and the CHAOS-8.5 global model are small, indicating good overall agreement and limited edge effects at ground level.

- A key finding is that the fastest decrease in total magnetic field does not occur at the current position of the second minimum ($0.56°W, 40.60°S$), but at a nearby position ($4.56°E, 32.62°S$). A similar behaviour is observed for the first minimum ($59.70°W, 26.30°S$), where the strongest field change is not collocated with the minimum itself, but instead found at approximately ($89.96°W, 48.98°S$). These positions were determined by generating a fine spatial grid with a resolution of $0.02° \text{ X } 0.02°$ in longitude and latitude. The tracking uncertainty is therefore controlled by the grid spacing, and the positional error is estimated to be $\pm 0.02°$.

- Finally, the interaction between the two SAA minima and their respective roles in the evolution of the SAA remain important topics for further investigation. Continued monitoring using updated satellite and ground-based observations, extension of the regional model in time and space, and detailed analysis of migration rates and intensity change will be essential to fully understand the dynamics of the SAA.

Acknowledgments

➢ The authors gratefully acknowledge the European Space Agency (ESA) for providing the *Swarm* satellite data, the International Service of Geomagnetic Indices (ISGI) for the geomagnetic indices used in this study, the INTERMAGNET network for the ground-based geomagnetic observatory data, and the South African National Space Agency (SANSA) for the repeat station data.

References

Gubbins, D., Barber, C.N., Gibbons, S., Love, J.J., (2000). Kinematic dynamo action in a sphere. I. Effects of differential rotation and meridional circulation on solutions with axial dipole symmetry. doi:10.1098/rspa.2000.0565.

Gubbins, D., Barber, C.N., Gibbons, S., Love, J.J., (2000). Kinematic dynamo action in a sphere. II. Symmetry selection. The Royal Society, 456(1999), 1333-1353. doi:10.1098/rspa.2000.0581.

Rother, M., Korte, M., Morschhauser, A., Vervelidou, F., Matzka, J., & Stolle, C. (2021). The mag.num core field model as a parent for IGRF-13, and the recent evolution of the South Atlantic Anomaly. doi:10.1186/s40623-020-01277-0.

Thébault, E., Schott, J. J., Mandea, M. (2006). Revised spherical cap harmonic analysis (R-SCHA): Validation and properties, doi:10.1029/2005JB003836.

Maus, S. (2010). Magnetic field model MF7. CIRES, Colo.

Finlay, C.C., Kloss, C., Olsen, N., Hammer, M.D., (2020). The CHAOS-7 geomagnetic field model and observed changes in the South Atlantic Anomaly. Earth Planets Space, 72, 1-31. doi:10.1186/s40623-020-01252-9.

Olsen, N., Friis-Christensen, E., (2013). The Swarm Satellite Constellation Application and Research Facility (SCARF) and Swarm data products. Earth Planet Space, 65, 1. doi:10.5047/eps.2013.07.001.

Courtillot, V., Ducruix, J., and LeMouël, J.L., 1978. Sur une accélération récente de la variation séculaire du champ magnétique terrestre. Comptes Rendus De l'Académie Des Sciences, 287:1095–1098.

Chulliat, A., Thébault, E., and Hulot, G., 2010. Core field acceleration pulse as a common cause of the 2003 and 2007 geomagnetic jerks, Geophys. Res. Lett., 37, L07301. https://doi.org/10.1029/2009GL042019.

References (cont.)

Khanyile, S.L., and Nahayo, E., 2024. Geomagnetic jerks observed in geomagnetic observatory data over southern Africa between 2017 and 2023. South African Journal of Geology, 127(1), 131-136. https://doi.org/10.25131/sajg.127.0019.

Khanyile, S.L., Nahayo, E., Pavȯn-Carrasco, F.J., Puente-Borque, M., 2026. Modelling earth's magnetic field over southern Africa between 2014 and 2023 applying revised spherical cap harmonic analysis (R-SCHA) on Swarm satellite and ground-based data. Physics of the Earth and Planetary Interiors, 372, 0031-9201. https://doi.org/10.1016/j.pepi.2026.107504.

Nahayo, E., Korte, M., 2022. A regional geomagnetic field model over Southern Africa derived with harmonic splines from Swarm satellite and ground-based data recorded between 2014 and 2019. Earth Planets Space 74, 8 (2022). https://doi.org/10.1186/s40623-021-01563-5.

Kloss, C., Finlay, C.C., Olsen, N., Tøffner-Clausen, L., Gillet, N., Grayver, A., 2024. The DTU geomagnetic field parent model and derived IGRF-14 candidate models. https://doi.org/10.5194/egusphere-egu25-3566.

Pavȯn-Carrasco, F. J., Marsal, S, Campuzano, S. A., and Torta, J. M., 2021. Signs of a new geomagnetic jerk between 2019 and 2020 from swarm and observatory data. Earth, Planet and Space 73(1):1-11. https://doi.org/10.1186/s40623-021-01504-2.

Smith, R., Rost, S., and Nowacki, A., 2016. The African Large Low Shear Velocity Province: Boundary Positions and Anisotropy Measurements. AGU Fall Meeting Abstracts, DI41C–2643. https://ui.adsabs.harvard.edu/abs/2016AGUFMDI41C2643S/abstract.

THANK YOU

www.sansa.org.za

@SANSA7

South African National Space Agency

South African National Space Agency

South African National Space Agency (SANSA)